Advances in Concrete Construction, *Vol. 13, No. 3 (2022) 223-231*
https://doi.org/10.12989/acc.2022.13.3.223

A system of several fraction laws for the identification of rotating response of FG shell

Ahmad Yahya[1], Muzamal Hussain*[2], Mohamed A. Khadimallah[3,4], Khaled Mohamed Khedher[5,6], K.S. Al-Basyouni[7], Emad Ghandourah[1], Essam Mohammed Banoqitah[1] and Adil Alshoaibi[8]

[1]*Nuclear Engineering Department, Faculty of Engineering, King Abdulaziz University, Jeddah P.O.Box 80204, Jeddah 21589, Saudi Arabia*
[2]*Department of Mathematics, Govt. College University Faisalabad, 38000, Faisalabad, Pakistan*
[3]*Civil Engineering Department, College of Engineering, Prince Sattam Bin Abdulaziz University, BP 655, Al-Kharj, 16273, Saudi Arabia*
[4]*Laboratory of Systems and Applied Mechanics, Polytechnic School of Tunisia, University of Carthage, Tunis, Tunisia*
[5]*Department of Civil Engineering, College of Engineering, King Khalid University, Abha 61421, Saudi Arabia*
[6]*Department of Civil Engineering, High Institute of Technological Studies, Mrezgua University Campus, Nabeul 8000, Tunisia*
[7]*Mathematics Department, Faculty of Science, King Abdulaziz University, Jeddah, Saudi Arabia*
[8]*Department of Physics, College of Science, King Faisal University, Al-Hassa, P.O. Box 400, Hofuf 31982, Saudi Arabia*

(*Received June 11, 2021, Revised March 5, 2022, Accepted March 10, 2022*)

Abstract. The problem is formulated by applying the Kirchhoff's conception for shell theory. The longitudinal modal displacement functions are assessed by characteristic beam ones meet clamped-clamped end conditions applied at the shell edges. The fundamental natural frequency of rotating functionally graded cylindrical shells of different parameter versus ratios of length-to-diameter and height-to-diameter for a wide range has been reported and investigated through the study with fractions laws. The frequency first increases and gain maximum value with the increase of circumferential wave mode. By increasing different value of height-to-radius ratio, the resulting backward and forward frequencies increase and frequencies decrease on increasing height-to-radius ratio. Moreover, on increasing the rotating speed, the backward frequencies increases and forward frequencies decreases. The trigonometric frequencies are lower than that of exponential and polynomial frequencies. Stability of a cylindrical shell depends highly on these aspects of material. More the shell material sustains a load due to physical situations, the more the shell is stable. Any predicted fatigue due to burden of vibrations is evaded by estimating their dynamical aspects.

Keywords: cylindrical shell; Kirchhoff's conception; polynomial; strain, stainless steel

1. Introduction

For theoretical vibration study of rotating cylindrical shell, the shells are supposed to be constructed from FG materials. Material composition along the radial direction is managed by a volume fraction law. The material stiffness moduli are written in integral forms and their integrands: geometrical parameters which are functions of the shell thickness variable. Vibration investigation of static and rotating cylindrical shells is a significant discipline in theoretical and applied mechanics. These shells have wide applications in engineering science and technology. For example, their uses are observed in civil, mechanical, electrical, nuclear engineering, aerodynamics, missile technology etc. More than one type of materials is used to structure the functionally graded materials and their physical properties vary from one surface to the other surface. In these surfaces, one has highly heat resistance property while other may preserve great dynamical perseverance and differs mechanically and physically in regular manner from one surface to other surface, making them of dual physical appearance. All these materials have changeable outer and inner sides and their physical properties greatly differ from each other (Suresh and Mortense 1997, Koizumi 1997). These materials are organized by various techniques and their applications are seen in dynamical elements such as plates, beams and shells. Moreover, they are also observed in space crafts, nuclear reactors and missiles technology etc.

Bryan (1890) is considered to be the primer research worker who examined studied vibrations of rotating cylindrical shells. The free vibrations of a rotating ring were related with those of these shells. Sharma *et al.* (1998) determined frequencies of composite cylindrical shells containing fluid. They estimated the axial modal deformations by trigonometric functions. Mehar *et al.* (2016) investigated the free vibration behavior of functionally graded carbon nanotube reinforced composite plate is investigated under elevated thermal environment. The carbon nanotube reinforced composite plate has been modeled mathematically using higher order shear deformation theory. The material properties of carbon nanotube reinforced composite plate are assumed to be temperature dependent and graded in the thickness direction using different grading rules. Di Taranto and Lessen (1964) investigated the vibrations of thin isotropic and infinite long

*Corresponding author, Ph.D.
Email: muzamal45@gmail.com,
muzamalhussain@gcuf.edu.pk

ISSN: 2287-5301 (Print), 2287-531X (Online)

rotating cylindrical shells. Sharma (1974) analyzed vibration frequencies circular cylinder with using the Rayleigh-Ritz formulation and made comparisons of his results with some experimental ones. Srinivasan and Lauterbach (1971) conducted the research on isotropic long rotating cylindrical shells including influence of coriolis actions on their travelling modes. Kar and Panda (2016) presented the free vibration responses of shear deformable functionally graded single/doubly curved panels under uniform, linear and nonlinear temperature fields. The micromechanical material model of functionally graded material is computed using Voigt model in conjunction with the power-law distribution to achieve the continuous gradation. The material properties are assumed to be the function of temperatures. Chung *et al.* (1981) studied the frequency response of fluid-filled CSs and presented an analysis of experimental and analytical investigation. Penzes and Kraus (1972) applied generalized end conditions to analyze vibrations of rotating cylindrical shells. The analysis of rotating shells was confined to some special cases owing to need of approximate approach and calculation process. With powerful numerical methodologies, shell vibration analysis has completely revolutionized by advanced computers. Sewall and Naumann (1968) considered the vibration analysis of CSs based on analytical and experimental methods. The shells were strengthened with longitudinal stiffeners. Kar and Panda (2017) examined the buckling and post buckling behavior of functionally graded spherical shell panel under nonuniform thermal environment. The effective material properties of the graded structure are evaluated using the Voigt's micromechanical model through the power-law distribution. For the analysis purpose, a general nonlinear higher order mathematical model is developed in conjunction with Green-Lagrange geometrical nonlinearity. Zohar and Aboudi (1973) studied vibrations of rotating cylindrical shells having finite length and matrix approach was used to derive the shell vibration. Kar and Panda (2017) studied the large amplitude flexural behaviour of functionally graded doubly curved shell panel is investigated numerically under the thermomechanical load. The nonlinear mathematical model of doubly curved shell panel is developed first time based on higher-order shear deformation theory and Green-Lagrange geometrical nonlinearity. In order to achieve the exact flexure of the structure, all the nonlinear higher order terms are included in the mathematical model. Najafizadeh and Isvandzibaei (2007) applied ring supports to CSs for vibration analysis of along the tangential direction and founded their research on angular deformation theory of higher order. The angular deformation was used for shell equations and determined the effects of constituent volume fractions and shell configurations on the shell vibrations. FG material parameters were changed step by step. Akbaş (2017a, b) investigated the forced vibration analysis of a cracked functionally graded microbeam using modified couple stress theory with damping effect. Mechanical properties of the functionally graded beam change vary along the thickness direction. The crack is modelled with a rotational spring. The Kelvin-Voigt model is considered in the damping effect. static bending of an edge cracked cantilever nanobeam composed of functionally graded material (FGM) subjected to transversal point load at the free end of the beam is investigated based on modified couple stress theory. Material properties of the beam change in the height direction according to exponential distributions. Wang and Chen (1974) performed frequencies of rotating cylindrical shells based on energy variational approach. Ergin and Temarel (2002) did a vibration study of cylindrical shells. The shells lied in a horizontal direction and contained fluid and submerged in it.

Kar and Panda (2016) investigated the post-buckling behaviour of functionally graded curved shell panels of different shell geometries (spherical, elliptical, cylindrical and hyperbolic) under the uniaxial and the biaxial edge compression. The inhomogeneity of the functionally graded material along the thickness direction is achieved using power-law distribution through Voigt's micromechanical model to obtain the effective material properties. The cracked beam is modelled using a proper modification of the classical cracked-beam theory consisting of two sub-beams connected through a massless elastic rotational spring. Akbaş (2017a, b) investigated the free vibration analysis of edge cracked cantilever microscale beams composed of functionally graded material (FGM) based on the modified couple stress theory (MCST). The material properties of the beam are assumed to change in the height direction according to the exponential distribution. The FG nanobeam is excited by a transverse triangular force impulse modulated by a harmonic motion. Mechanical properties of FG beam depend on the position. The Kelvin-Voigt model is considered in the damping effect. In solution of the dynamic problem, finite element method is used within Timoshenko beam theory.

Akbaş (2018) presented the forced vibration responses of a cantilever nanobeam with crack using modified couple stress theory with damping effect. The crack is modeled with a rotational spring. The Kelvin-Voigt model is considered in the damping effect. In solution of the dynamic problem, finite element method is used within Timoshenko beam theory in the time domain. Influences of the geometry, crack and material parameters on forced vibration responses of cracked nanobeams are examined and discussed. Ramteke *et al.* (2021) obtained the finite element solutions of static deflection and stress values for the functionally graded structure considering variable grading patterns (power-law, sigmoid and exponential) including the porosity effect. The unknown values are obtained computationally via a customized computer code with the help of cubic-order displacement functions considering the varied distribution of porosity (even and uneven) through the panel thickness. Padovan (1975) did analysis of pre-stress influence on buckling and vibration aspects of rotating cylindrical shells. Akbaş (2019) presented axially forced vibration of a cracked nanorod under harmonic external dynamically load. In constitutive equation of problem, the nonlocal elasticity theory is used. The Crack is modelled as an axial spring in the crack section. In the axial spring model, the nonrod separates two sub-nanorods and the flexibility of the axial spring represents the effect of the crack. Boundary condition of the nanorod is selected as fixed-free and a harmonic load is subjected at the free end of the nanorod. Ramteke *et al.* (2020) studied two directional graded structure has been developed using a commercial FE package ANSYS and the subsequent deflection responses are obtained. Additionally, the model includes the porosity within the graded structure considering even type of distribution pattern. The present model is derived using the basic steps available in the ANSYS platform through the batch input technique. Goncalves and Batista (1987) gave an analytical investigation of submerged CSs with fluid. Ramteke (2019) developed a geometrical model for the analysis and modelling of the uniaxial functionally graded structure using the higher-order displacement kinematics with and without the presence of porosity including the distribution. Additionally, the formulation is capable of modelling three different kinds of grading patterns i.e., Power-law, sigmoid and exponential distribution of the individual constituents through the thickness direction. Fox and Hardie (1985) examined vibrations of rotating cylindrical shells. They used shell theory due to Flugge for shell motion equations. Akbaş (2020) investigated the axially damped forced vibration responses of viscoelastic nanorods within the frame of the modal analysis. The nonlocal elasticity theory is used in the constitutive relation of the nanorod with the Kelvin-Voigt viscoelastic model. In the forced vibration problem, a cantilever nanorod subjected to a harmonic load at the free end of the nanorod is considered in the numerical examples. Amabili *et al.* (1999) used Donnell's shallow-shell model with the quiescent, dense, inviscid and incompressible fluid. Also the dense fluid is studied for the influence of both the internal and external side of the shell. In the external side of the shell, the fluid was considered as an unbounded domain in the radial direction, while internally, the shell was considered as filled completely. The shell motion equations were used for rotating cylindrical shell by different researchers (Saito and Endo 1996, Wang and Sivadas and Ganesan 1994, Chen *et al.* (1993). Civalek (2020) presented the free vibration characteristics of thick skew plates reinforced by functionally graded carbon nanotubes (CNTs) reinforced composite. Discrete singular convolution (DSC) method is used for the numerical solution of vibration problems via geometric mapping technique. Using the geometric transformation via a four-node element, the straight-sided quadrilateral physical domain is mapped into a square domain in the computational space. Lam and Loy (1994) investigated the vibrations of rotating composite and sandwich cylindrical shells. They performed comparisons of vibration frequencies of composited rotating cylindrical shells and evaluated the results applying different shell theories. Civalek and Jalaei (2020) studied a geometric transformation method based on discrete singular convolution (DSC) to solve the buckling problem of a functionally graded carbon nanotube (FG-CNT)-reinforced composite skew plate. The straight-sided quadrilateral plate geometry is mapped into a square domain in the computational space using a four-node DSC transformation method. Akbaş (2016a, b) studied the forced vibration analysis of a simple supported viscoelastic nanobeam based on modified couple stress theory (MCST). The nanobeam is excited by a transverse triangular force impulse modulated by a harmonic motion. The elastic medium is considered as Winkler-Pasternak elastic foundation. The damping effect is considered by using the Kelvin-Voigt viscoelastic model. Pankaj *et al.* (2019) studied the functionally graded material using sigmoid law distribution under hygrothermal effect. Frequency spectra for aspect ratios have been depicted according to various edge conditions. Li and Lam (1998) studied influence of edge conditions vibration frequencies and modes of rotating composite CSs. Several researchers used different approaches for the investigation of frequency of cylinders and concrete material (Kagimoto *et al.* 2015, Mesbah and Benzaid 2017, Alijani and Bidgoli 2018, Demir and Livaoglu 2019, Samadvand and Dehestani 2020, Ramteke *et al.* 2020, Ramteke and Panda 2021, Mehar and Panda 2018).

In present paper, vibrations of rotating FG-CSs have been analyzed with clamped-clamped with different law index. The governing equation has been developed for the vibrations of FG-CSs considering the various power law indexes. Also the rotating frequency characteristics of shell for different geometrical parameters (ratios of thickness-to-radius and length-to-radius) is either not established or assumed very little attention. Functionally graded materials are assumed to be structured them. Dynamical behavior of a cylindrical shell is described with regard to the reference surface, length, radius and thickness quantities and boundary conditions applied its ends. For motion of a static cylindrical shell, a stationary wave is generated due to vibration. Moreover, on increasing the rotating speed, the backward frequencies increases and forward frequencies decreases.

2. Mathematical formulation

The motion of cylindrical shell predominates the resultant forces and moments so expressions for these forces are written as

$$\{N_{xx}, N_{\theta\theta}, N_{x\theta}\} - \nabla^2\{N_{xx}, N_{\theta\theta}, N_{x\theta}\} = \int_{\frac{-h}{2}}^{\frac{h}{2}} (\tilde{\sigma}_{xx}, \tilde{\sigma}_{\theta\theta}, \tilde{\sigma}_{x\theta})dz \tag{1}$$

$$\{M_{xx}, M_{\theta\theta}, M_{x\theta}\} - \nabla^2\{M_{xx}, M_{\theta\theta}, M_{x\theta}\} = \int_{\frac{-h}{2}}^{\frac{h}{2}} (\tilde{\sigma}_{xx}, \tilde{\sigma}_{\theta\theta}, \tilde{\sigma}_{x\theta})zdz \tag{2}$$

here $\tilde{\sigma}_{xx}$ and $\tilde{\sigma}_{\theta\theta}$ stands for stress factors along the axial and tangential directions respectively and $\tilde{\sigma}_{x\theta}$ indicates the shear stress in $x\theta$-plane.

The stress element from Hooke's law can be written as

$$\begin{pmatrix} \tilde{\sigma}_{xx} \\ \tilde{\sigma}_{\theta\theta} \\ \tilde{\sigma}_{x\theta} \end{pmatrix} - \nabla^2 \begin{pmatrix} \tilde{\sigma}_{xx} \\ \tilde{\sigma}_{\theta\theta} \\ \tilde{\sigma}_{x\theta} \end{pmatrix} = \begin{bmatrix} \hat{Q}_{11} & \hat{Q}_{12} & 0 \\ \hat{Q}_{12} & \hat{Q}_{22} & 0 \\ 0 & 0 & \hat{Q}_{66} \end{bmatrix} \begin{pmatrix} e_{xx} \\ e_{\theta\theta} \\ e_{x\theta} \end{pmatrix} \tag{3}$$

In same manner e_{xx} and $e_{\theta\theta}$ exhibit the strain in x- and θ-directions and $e_{x\theta}$ presents the shear strain in the $x\,\theta$-plane.

For FG-CSs, $\hat{Q}_{kl}\ (k,l=1,2,\ldots 6)$ symbolizes tis termed as

$$\hat{Q}_{11}=\frac{E}{1-\nu^2}=\hat{Q}_{22},\hat{Q}_{12}=\frac{\nu E}{1-\nu^2}=\hat{Q}_{21},\quad \hat{Q}_{66}=\frac{E}{2(1+\nu)} \tag{4}$$

Love (1952) submitted the first thin shell theory on base of Kirchhoff's conception. Moreover, an additional modified form of thin shell theory (1963) is established. The components of the strain vector (e) in Eq. (3), that are considered by Love (1952) can be expressed as linear combinations

$$e_{xx}=e_{11}+z\kappa_{11},\ e_{\theta\theta}=e_{22}+z\kappa_{22},\quad e_{x\theta}=e_{12}+2z\kappa_{12} \tag{5}$$

κ_{11}, κ_{22}, and κ_{12} are known as surface curvatures whereas e_{11}, e_{22} and e_{12} signify the reference surface strains.

Since from Love's theory, the expressions of relation between strain and curvature displacement functions are considered as

$$[e_{11},e_{22},e_{12}]=\left[\frac{\partial u}{\partial x},\frac{1}{R}\left(\frac{\partial v}{\partial\theta}+w\right),\left(\frac{\partial v}{\partial x}+\frac{1}{R}\frac{\partial u}{\partial\theta}\right)\right]$$
$$[\kappa_{11},\kappa_{22},\kappa_{12}]=\begin{bmatrix}-\frac{\partial^2 w}{\partial x^2},-\frac{1}{R^2}\left(\frac{\partial^2 w}{\partial\theta^2}-\frac{\partial v}{\partial\theta}\right),\\ -\frac{2}{R}\left(\frac{\partial^2 w}{\partial x\partial\theta}-\frac{3}{4}\frac{\partial v}{\partial x}+\frac{1}{4R}\frac{\partial u}{\partial\theta}\right)\end{bmatrix} \tag{6}$$

By substituting Eqs. (3)-(6), resultant forces and moments takes the following form

$$N_{xx}-\nabla^2 N_{xx}=\int_{\frac{-h}{2}}^{\frac{h}{2}}\tilde{\sigma}_{xx}dz=\frac{Eh}{1-\nu^2}\frac{\partial u}{\partial x}+\frac{\nu Eh}{1-\nu^2}\frac{1}{R}(\frac{\partial v}{\partial\theta}+w) \tag{7a}$$

$$N_{\theta\theta}-\nabla^2 N_{\theta\theta}=\int_{\frac{-h}{2}}^{\frac{h}{2}}\tilde{\sigma}_{\theta\theta}dz=\frac{\nu Eh}{1-\nu^2}\frac{\partial u}{\partial x}+\frac{Eh}{1-\nu^2}\frac{1}{R}(\frac{\partial v}{\partial\theta}+w) \tag{7b}$$

$$N_{x\theta}-\nabla^2 N_{x\theta}=\int_{\frac{-h}{2}}^{\frac{h}{2}}\tilde{\sigma}_{x\theta}dz=\frac{Eh}{2(1+\nu)}(\frac{1}{R}\frac{\partial u}{\partial x}+\frac{\partial v}{\partial\theta}) \tag{7c}$$

$$M_{xx}-\nabla^2 M_{xx}=\int_{\frac{-h}{2}}^{\frac{h}{2}}\tilde{\sigma}_{xx}dz=\frac{\nu D}{R^2}\frac{\partial v}{\partial\theta}-D(\frac{\nu}{R^2}\frac{\partial^2 w}{\partial\theta^2}+\frac{\partial^2 w}{\partial x^2}) \tag{7d}$$

$$M_{\theta\theta}-\nabla^2 M_{\theta\theta}=\int_{\frac{-h}{2}}^{\frac{h}{2}}\tilde{\sigma}_{\theta\theta}dz=\frac{D}{R^2}\frac{\partial v}{\partial\theta}-D(\frac{1}{R^2}\frac{\partial^2 w}{\partial\theta^2}+\nu\frac{\partial^2 w}{\partial x^2}) \tag{7e}$$

$$M_{x\theta}-\nabla^2 M_{x\theta}=\int_{\frac{-h}{2}}^{\frac{h}{2}}\tilde{\sigma}_{x\theta}zdz=D\frac{(1-\nu)}{R}(\frac{\partial u}{\partial\theta}+\frac{3}{4}\frac{\partial v}{\partial x}-\frac{\partial^2 w}{\partial\theta\partial x}) \tag{7f}$$

Meanwhile $D=\frac{Eh^3}{12(1-\nu^2)}$ refers as bending rigidity of shell.

The mass density per unit length ρ_t is defined as

$$\rho_t=\int_{\frac{-h}{2}}^{\frac{h}{2}}\rho dz \tag{8}$$

while ρ entitles as mass density.

The fundamental equations from the Love shell theory (1952) are considered as

$$\begin{aligned}&\frac{\partial N_{xx}}{\partial x}+\frac{1}{R}\frac{\partial N_{x\theta}}{\partial\theta}-\frac{1}{2R^2}\frac{\partial M_{x\theta}}{\partial\theta}=\rho_t\frac{\partial^2 u}{\partial^2 t}\\&\frac{1}{R}\frac{\partial N_{\theta\theta}}{\partial\theta}+\frac{\partial N_{x\theta}}{\partial x}+\frac{1}{R^2}\frac{\partial M_{\theta\theta}}{\partial\theta}+\frac{3}{2R}\frac{\partial M_{x\theta}}{\partial x}=\\&\rho_t\left(\frac{\partial^2 v}{\partial^2 t}+\psi\frac{\partial w}{\partial t}-\psi^2 v\right)\\&\frac{\partial^2 M_{xx}}{\partial x^2}+\frac{1}{R^2}\frac{\partial^2 M_{\theta\theta}}{\partial^2\theta}+\frac{2}{R}\frac{\partial^2 M_{x\theta}}{\partial\theta\partial x}-\frac{N_{\theta\theta}}{R}+p=\\&\rho_t\left(\frac{\partial^2 w}{\partial^2 t}-\psi\frac{\partial v}{\partial t}-\psi^2 v\right)\end{aligned} \tag{9}$$

where ρ expresses the applied pressure on the shell.

3. Volume fraction laws

Vibrations of rotating FG circular cylindrical shells are inspected for three volume fraction laws viz.: polynomial, exponential and trigonometric. These laws control functionally graded material composition in the shell radius direction. The term V_f is designated as total volume fraction of FG-CS, respectively. The power exponent is denoted as Γ and h for thickness and z is the coordinate which varies from zero to infinity

$$V_f=\left(\frac{z}{h}+\frac{1}{2}\right)^{\eta} \tag{10}$$

On mixing two or more than two materials like nickel and stainless steel, functionally graded materials are obtained. These shells are classified into two kinds depending on the order of constituent materials. Their arrangement has profound influence on the formation of FG-CSs. The order of the FG constituent materials is reversed as Type-I and Type-II. At temperature 300K, the material properties for FG-CS are: E, υ, ρ for Stainless steel are $2.077882\times10^{11}\ \frac{N}{m^2}$, 0.317756 and 8166 $\frac{Kg}{m^3}$ and Nickel are $2.05098\times10^{11}\ \frac{N}{m^2}$, 0.3100, and 8900 $\frac{Kg}{m^3}$.

So the Young's modulus E_{fgm}, Poisson ratio v_{fgm} and mass density ρ_{fgm} for three different laws are defined as: FGM Polynomial Law (Law-I)

$$\rho = (\rho_1 - \rho_2)\left(\frac{z}{h} + 0.5\right)^{\eta} + \rho_2 \tag{11}$$

FGM Exponential Law (Law-II)

$$E = (E_1 - E_2)\left(1 - e^{-\left(\frac{2}{h}+\frac{1}{2}\right)^{\eta}}\right) + E_2 \tag{12}$$

FGM Trigonometric Law (Law-III)

$$v = (v_1 - v_2)\, sin^2\left[\left(\frac{2}{h} + \frac{1}{2}\right)^{\eta}\right] + v_2 \tag{13}$$

In Eqs. (11)-(13), other physical parameter can be written same. When $z = -\frac{h}{2}$ is substituted in the Eqs. (8)-(13), $E = E_2$, $v = v_2$ and $\rho = \rho_2$ which are material properties of Type-I and when substitution $z = \frac{h}{2}$ is made in the above expressions, $E = E_1$, $v = v_1$ and $\rho = \rho_1$ for a Type-II. These substitutions show that there is an incessant change of fabric properties of the fabric Type-I at the shell internal surface to those of the fabric Type-II, at the shell external surface where $z = 0$ is associated to its mid surface. A FG-CS comprised of two materials is heterogeneous shell and its vibration characteristics are can be studied by applying any appropriate thin shell theory provided its radius to thickness ratio is greater than twenty. During the past few years, numerous theories have been extensively debated for vibration of nanotube, shell and plate morphologies of several conformations depending upon certain edge conditions. Wave propagation approach is among the most significant and successfully used numerical technique by researchers to investigate the free vibrations of cylinder-shaped shell, plates and nanotubes. The three modal displacement functions of the shell for ith tube can be written as

$$u^{(i)} = a_m\, cos(n\theta) e^{(i\omega t - ik_m x)} \tag{14a}$$

$$v^{(i)} = b_m\, sin(n\theta) e^{(i\omega t - ik_m x)} \tag{14b}$$

$$w^{(i)} = c_m\, cos(n\theta) e^{(i\omega t - ik_m x)} \tag{14c}$$

where a_m, b_m, c_m describe the displacement amplitude coefficients in x, θ and z directions correspondingly. The angular frequency is designated as ω, circumferential wave number by n and k_m referred to be axial wave number allied with end supports obligatory on FG-CSs. After putting the Eqs. (14a)-(14c) into Eq. (9), we get a frequency equation in Eigen value form.

4. Result and discussion

For a system of multiple fraction laws, the present model is based on the Kirchhoff's conception. The vibrational response has been demonstrated and verified with results presented in the literature. Considering the negligible percentage of error, thus it confirms the validation of suggested shell model. Some numerical results are evaluated for isotropic cylindrical shell for comparing with existing results found in the literature. The present model can be easily reduced to the isotropic one by considering suitable material parameter for isotropic tube. Hence the present model holds good agreement with the existing results (Moazzez *et al.* 2018, Zhang *et al.* 200) for isotropic tubes as seen in Tables 1 and 2. Table 3 shows the rotating frequencies versus *n* (wave number) and *m* (axial wave mode) for both Types (I and II). The frequencies for backward and forward waves increase indefinitely as *n* and *m* grows for FG-CSs. Moreover, the order of constituent material of the shell impresses the frequency values.

Table 1 Comparison for isotropic cylindrical shell with Moazzez *et al.* (2018)

m	Method	n				
		1	2	3	4	5
1	Moazzez *et al.* (2018)	3.81	10.87	22.02	39.00	61.21
	Present	3.86	10.91	22.19	39.29	61.43

Table 2 Convergence of present method frequencies (Zhang *et al.* 2001)

Method	Modal order (*m*, *n*)			
	(1,3)	(2,3)	(3,3)	(3,4)
Zhang *et al.* (2001)	8.94	10.64	14.66	19.96
Present	8.90	10.62	14.59	19.85
Zhang *et al.* (2001)	19.61	23.28	31.98	39.78
Present	19.6	23.31	32.01	39.81

Table 3 Rotating FGM Type-I and-II frequency variation of versus, ψ (n=2, η=0.7, L=5 m, h=0.003 m, R=1 m)

m			ψ				
			0.1	0.2	0.3	0.4	0.5
Type-I	1	Backward	38.917	39.017	39.120	39.227	39.336
		Forward	38.726	40.634	38.546	38.461	38.379
Type-II	1	backward	38.953	41.053	42.156	42.263	38.372
		forward	38.810	38.670	42.582	42.497	38.414

Table 4 Rotating FGM Type-I frequency variation of versus, *h*/*R*: (*m*=1, *L*/*R*=15, η=0.5, *n*=2, ψ=3)

h/R	Polynomial		Exponential		Trigonometric	
	Backward	Forward	Backward	Forward	Backward	Forward
0.001	10.463	9.6999	10.445	9.6811	10.427	9.6623
0.002	15.522	14.758	15.495	14.731	15.477	14.713
0.003	21.398	20.634	21.361	20.597	21.343	20.409
0.004	27.564	26.800	27.518	26.753	27.501	26.565
0.005	33.859	33.095	33.803	33.039	33.803	32.851
0.006	40.222	39.457	40.155	39.391	40.137	39.203
0.007	46.621	45.857	46.545	45.780	46.527	45.592
0.008	53.044	52.279	52.957	52.192	52.939	52.004
0.009	59.480	58.715	59.383	58.618	59.365	58.430
0.01	65.924	65.159	65.817	65.052	65.796	64.864

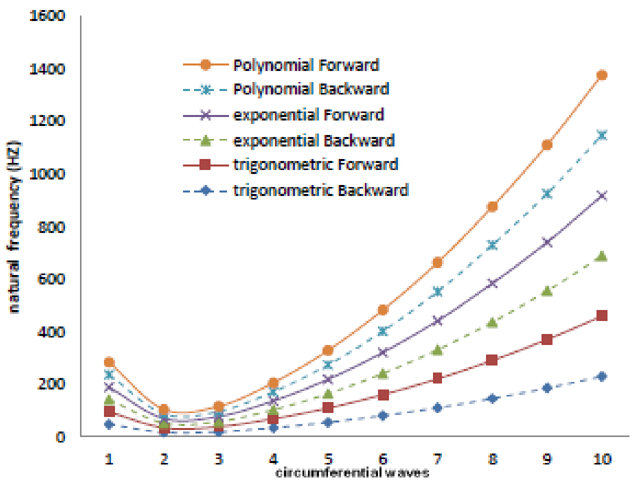

Fig. 1 The backward and forward Type-I C-C frequencies against *n: (m*=1, *h*/*R*=0.03, *L*/*R*=10, *ψ*=1, *η*=30)

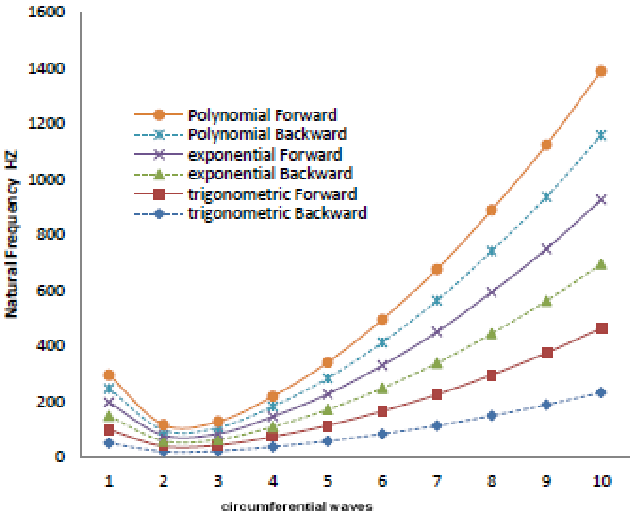

Fig. 2 The backward and forward Type-I C-C frequencies against *n: (m*=1, *h*/*R*=0.03, *L*/*R*=10, *η*=30)

Tables 4 and 5 shows the frequency value w.r.t *h/R*. The frequency values increase on increasing *h/R* for Types (I and II). The polynomial frequencies are higher than that of other two laws. It is also exhibited that the frequencies of Type-I is less than that of Type-II. Figs. 1 and 2 shows the variations of Type-I and -II frequencies with clamped-clamped (C-C) end condition versus *n*. The material work of the shell is restricted by three volume fraction laws: (I), (II), (III). It shows that frequency determined by the polynomial law is the higher than that calculated from other two laws. It shows that frequency determined by the trigonometric law is the higher than that evaluated from other two laws. In these figures, the natural frequencies (Hz) of a rotating functionally graded cylindrical shell drawing for the circumferential wave number *n*. The variation of frequencies have been established with the polynomial (Law-I), exponential (Law-II) and trigonometric (Law-III) which is called the volume fraction laws. Both backward and forward frequencies increase as their circumferential wave number *n* is increased. Tables 6 and 7 indicates the frequency pattern versus *ψ* (angular speed)

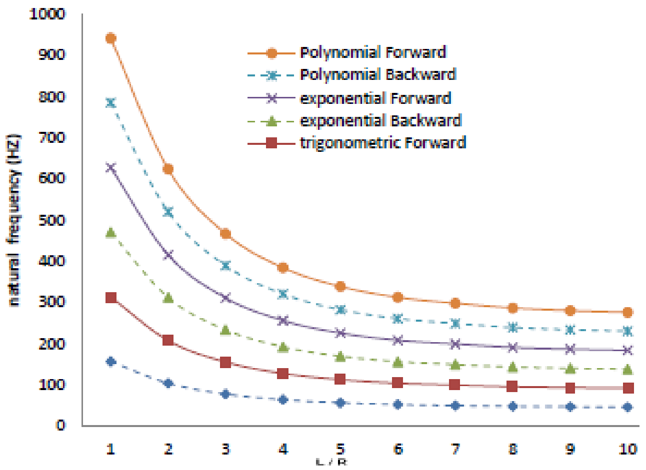

Fig. 3 The backward and forward Type-I C-C frequencies against *L*/*R*: *ν*=0.3, *m*=1, *h*/*R*=0.01, *η*=10, *n*=2, *ψ*=3)

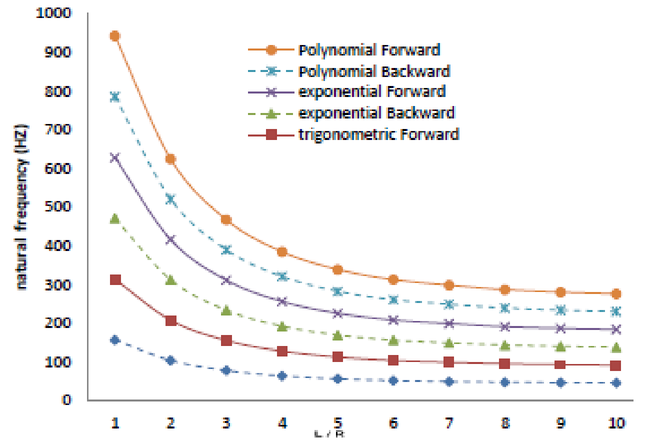

Fig. 4 The backward and forward Type-II C-C frequencies against *L*/*R*: *ν*=0.3, *m*=1, *h*/*R*=0.01, *η*=10, *n*=2, *ψ*=3)

Table 5 Rotating FGM Type-II frequency variation of versus, *h*/*R*: (*m*=1, *L*/*R*=10, *η*=0.7, *n*=2, *ψ*=3)

h/*R*	Polynomial		Exponential		Trigonometric	
	Backward	Forward	Backward	Forward	Backward	Forward
0.001	18.322	17.558	18.354	17.591	18.386	17.624
0.002	21.549	20.786	21.589	20.825	21.621	20.858
0.003	26.050	25.287	26.097	25.333	26.129	25.366
0.004	31.272	30.509	31.327	30.563	31.359	30.596
0.005	36.907	36.143	36.074	35.805	36.106	35.738
0.006	42.788	42.023	42.857	42.095	42.889	42.127
0.007	48.825	48.060	48.905	48.140	48.937	48.173
0.008	54.965	54.203	55.053	54.288	55.085	54.321
0.009	61.175	60.410	61.272	60.507	61.304	60.540
0.01	67.4343	66.669	67.540	66.775	67.572	66.808

for two rotating functionally graded cylindrical shells. The frequencies pattern observed different for backward and forward on increasing the rotation speed. When shell starts rotation from *ψ*=0, the backward and forward frequencies constant for Types (I and II). The backward frequencies of shell increases and forward frequencies decrease on increasing the rotation speed (Chen *et al.* 1993). The shape

Table 6 The natural frequencies (Hz) for C-C functionally graded cylindrical shell with angular speed ψ for Type I: (m=1, h/R=0.05, L/R=10, n=2, η=30)

Ω	Polynomial		Exponential		Trigonometric	
	Backward	Forward	Backward	Forward	Backward	Forward
0	25.633	25.583	25.403	25.301	25.163	25.101
1	25.939	25.244	26	25	25	25
2	26.209	24.999	25.912	24.732	25.632	24.522
3	26.506	24.7833	26.123	24.521	25.823	24.271
4	26.747	24.586	26.341	24.311	26.041	24.059
5	26.978	24.37	26.571	24.1091	26.221	23.841
6	27.199	24.1733	26.771	23.9051	26.391	23.641
7	27.43	23.9433	26.993	23.6833	26.599	23.433
8	27.668	23.753	27.173	23.5001	26.798	23.2293
9	27.893	23.563	27.395	23.3211	26.985	23.0651

Table 7 The natural frequencies (Hz) for C-C functionally graded cylindrical shell with angular speed ψ for Type II: (m=1, h/R=0.03, L/R=10, n=2, η=30)

Ω	Polynomial		Exponential		Trigonometric	
	Backward	Forward	Backward	Forward	Backward	Forward
0	11.163	11.102	11.402	11.302	11.624	11.582
1	11.407	11.782	12.678	11.992	11.932	11.243
2	11.632	10.523	11.913	10.731	12.178	10.998
3	11.821	10.272	12.122	10.522	12.414	10.7834
4	12.042	10.057	12.342	10.313	12.646	10.587
5	12.222	9.842	12.5714	10.1092	12.877	10.361
6	12.393	9.6421	12.775	9.9054	13.098	10.132
7	12.595	9.4332	12.992	9.6832	13.321	9.9434
8	12.799	9.2293	13.176	9.5006	13.567	9.752
9	12.985	9.0653	13.395	9.3212	13.794	9.5608

of the graph has a different style for backward and forward frequencies. Figs. 3 and 4 sketched for natural frequencies (Hz) for a rotating functionally graded cylindrical shell are sketched versus *L/R* for Type-I. As *L/R* is increased, the backward and forward frequencies (Hz) get lower down for all laws. As for the frequency variation behavior with the laws, both forward and backward frequencies are higher than those corresponding to other two laws. For the polynomial volume law, the forward and backward frequencies are the highest than those for other two laws. In Fig. 4, natural frequencies (Hz) for a rotating functionally graded cylindrical shell Type are sketched versus *L/R* for Type-II. As *L/R* is enhanced, the backward and forward frequencies (Hz) diminish for the three volume fraction laws. As for the frequency variation behavior with the laws, both forward and backward frequencies are higher than those corresponding to other two laws. For the trigonometric volume law, the forward and backward frequencies are the lowest than those for other two laws i.e., the polynomial and exponential.

5. Conclusions

Employment of the Kirchhoff's conception for shell theory gives birth to the shell frequency equation. Influence of functionally graded materials is examined on shell frequencies. Expressions for modal displacement functions, the three unknown functions are supposed in such way that the axial, circumferential and time variables are separated by the product method. Throughout the computation, clamped-clamped edge condition is used. To generate the fundamental natural frequencies and for better accuracy and effectiveness, the computer software MATLAB is used. The rotating frequencies of FG-shell with three fraction laws are investigated with circumferential wave number, length- and height-radius ratios. Moreover, the effect of height- and length-to-radius ratio is investigated. It is examined that the backward and forward frequencies increase and decrease on increasing the ratio of height- and length-to-radius ratio. It has been. It is found that the rotating frequencies of exponential law is sandwich between the polynomial and trigonometric laws. The present procedure can be protracted to perform vibration study of rotating fluid-filled carbon nanotubes with ring supports.

Declaration of conflicting interests

The author(s) declared no potential conflicts of interest with respect to the research, authorship, and/or publication of this article.

Acknowledgment

This project was funded by the Deanship of Scientific Research (DSR), King Abdulaziz University, Jeddah, under grant No. G: 158-135-1442. The authors, therefore, gratefully acknowledge DSR technical and financial support.

References

Ahmad, M. and Naeem, M.N. (2009), "Vibration characteristics of rotating FGM circular cylindrical shell using wave propagation method", *Europ. J. Sci. Res.*, **36**(2), 184-235.

Akbaş Ş.D. (2017a), "Free vibration of edge cracked functionally graded microscale beams based on the modified couple stress theory", *Int. J. Struct. Stability Dyn.*, **17**(3), 1750033. https://doi.org/10.1142/S021945541750033X.

Akbaş, Ş.D. (2016a), "Forced vibration analysis of viscoelastic nanobeams embedded in an elastic medium", *Smart Struct. Syst.*, **18**(6), 1125-1143. https://doi.org/10.12989/sss.2016.18.6.1125.

Akbaş, Ş.D. (2016b), "Analytical solutions for static bending of edge cracked micro beams", *Struct. Eng. Mech.*, **59**(3), 579-599. https://doi.org/10.12989/sem.2016.59.3.579.

Akbaş, Ş.D. (2017b), "Forced vibration analysis of functionally graded nanobeams", *Int. J. Appl. Mech.*, **9**(7), 1750100. https://doi.org/10.1142/S1758825117501009.

Akbaş, Ş.D. (2018), "Forced vibration analysis of cracked nanobeams", *J. Brazil. Soc. Mech. Sci. Eng.*, **40**(8), 1-11.

https://doi.org/10.1007/s40430-018-1315-1.
Akbas, S.D. (2018a), “Forced vibration analysis of cracked functionally graded microbeams”, *Adv. Nano Res.*, **6**(1), 39. https://doi.org/10.12989/anr.2018.6.1.039.
Akbaş, Ş.D. (2018b), “Bending of a cracked functionally graded nanobeam”, *Adv. Nano Res.*, **6**(3), 219. https://doi.org/10.12989/anr.2018.6.3.219.
Akbaş, Ş.D. (2019), “Axially forced vibration analysis of cracked a nanorod”, *J. Comput. Appl. Mech.*, **50**(1), 63-68. http://doi.org/10.22059/jcamech.2019.281285.392.
Akbaş, Ş.D. (2020), “Modal analysis of viscoelastic nanorods under an axially harmonic load”, *Adv. Nano Res.*, **8**(4), 277. https://doi.org/10.12989/anr.2020.8.4.277.
Alijani, M. and Bidgoli, M.R. (2018), “Agglomerated SiO2 nanoparticles reinforced-concrete foundations based on higher order shear deformation theory: Vibration analysis”, *Adv. Concrete Constr.*, **6**(6), 585. https://doi.org/10.12989/acc.2018.6.6.585.
Amabili, M., Pellicano, F. and Paidoussis M.P. (1998), “Nonlinear vibrations of simply Love, A.E.H. (1888), “On the small free vibrations and deformation of thin elastic shell”, *Phil. Trans. R. Soc. London*, **A179**, 491-549.
Bryan, G.H. (1890), “On the beats in the vibration of revolving cylinder”, *Proceedings of the Cambridge philosophical Society*, **7**, 101-111.
Chen, Y., Zhao, H.B. and Shin, Z.P. (1993), “Vibration of high speed rotating shells with calculation for cylindrical shells”, *J. Sound Vib.*, **160**, 137. https://doi.org/10.1006/jsvi.1993.1010.
Chung, H., Turula, P. Mulcahy, T.M. and Jendrzejczyk, J.A. (1981), “Analysis of cylindrical shell vibrating in a cylindrical fluid region”, *Nucl. Eng. Des.*, **63**(1), 109-1012. https://doi.org/10.1016/0029-5493(81)90020-0.
Civalek, Ö. (2020), “Vibration of functionally graded carbon nanotube reinforced quadrilateral plates using geometric transformation discrete singular convolution method”, *Int. J. Numer. Method. Eng.*, **121**(5), 990-1019. https://doi.org/10.1002/nme.6254.
Civalek, O. and Jalaei, M.H. (2020), “Buckling of carbon nanotube (CNT)-reinforced composite skew plates by the discrete singular convolution method”, *Acta Mechanica*, **231**(6), 2565-2587. https://doi.org/10.1007/s00707-020-02653-3.
Demir, A.D. and Livaoglu, R. (2019), “The role of slenderness on the seismic behavior of ground-supported cylindrical silos”, *Adv. Concrete Constr.*, **7**(2), 65. https://doi.org/10.12989/acc.2019.7.2.065.
Di Taranto, R.A. and Lessen, M. (1964), “Coriolis acceleration effect on the vibration of rotating thin-walled circular cylinder”, *Trans. ASME*, *J. Appl. Mech.*, **31**, 700-701. https://doi.org/10.1115/1.3629733.
Ergin, A. and Temarel, P. (2002), “Free vibration of a partially liquid-filled and submerged, horizontal cylindrical shell”, *J. Sound Vib.*, **254**(5), 951-965. https://doi.org/10.1006/jsvi.2001.4139.
Fox, C.H.J. and Hardie, D.J.W. (1985), “Harmonic response of rotating cylindrical shell”, *J. Sound Vib.*, **101**, 495. https://doi.org/10.1016/S0022-460X(85)80067-5.
Ghosh, A, Miyamoto, Y, Reimanis, I. and Lannutti, J.J. (1997), “Functionally graded materials, manufacture, properties and applications”, *Am. Ceram. Transac.*, **76**, 171-89.
Kagimoto, H., Yasuda, Y. and Kawamura, M. (2015), “Mechanisms of ASR surface cracking in a massive concrete cylinder”, *Adv. Concrete Constr.*, **3**(1), 039. https://doi.org/10.12989/acc.2015.3.1.039.
Kar, V.R. and Panda, S.K. (2015), “Free vibration responses of temperature dependent functionally graded curved panels under thermal environment”, *Latin Am. J. Solid. Struct.*, **12**(11), 2006-2024.
Kar, V.R. and Panda, S.K. (2015), “Thermoelastic analysis of functionally graded doubly curved shell panels using nonlinear finite element method”, *Compos. Struct.*, **129**, 202-212. https://doi.org/10.1016/j.compstruct.2015.04.006.
Kar, V.R. and Panda, S.K. (2016), “Post-buckling behaviour of shear deformable functionally graded curved shell panel under edge compression”, *Int. J. Mech. Sci.*, **115**, 318-324. https://doi.org/10.1016/j.ijmecsci.2016.07.014.
Kar, V.R. and Panda, S.K. (2017), “Postbuckling analysis of shear deformable FG shallow spherical shell panel under nonuniform thermal environment”, *J. Therm. Stress.*, **40**(1), 25-39. https://doi.org/10.1080/01495739.2016.1207118.
Koizumi, M. (1997), “FGM activities in Japan”, *Compos. Part B Eng.*, **28**(1-2), 1-4. https://doi.org/10.1016/S1359-8368(96)00016-9.
Lam K.Y. and Loy, C.T. (1994), “On vibration of thin rotating laminated composite cylindrical shells”, *J. Sound Vib.*, **116**, 198. https://doi.org/10.1016/0961-9526(95)91289-S.
Li, H. and Lam, K.Y. (1998), “Frequency characteristics of a thin rotating cylindrical shell using the generalized differential quadrature method”, *Int. J. Mech. Sci.*, **40**(5), 443-459. https://doi.org/10.1016/S0020-7403(97)00057-X.
Mehar, K. and Panda, S.K. (2018), “Elastic bending and stress analysis of carbon nanotube-reinforced composite plate: Experimental, numerical, and simulation”, *Adv. Polym. Tech.*, **37**(6), 1643-1657. https://doi.org/10.1002/adv.21821.
Mehar, K., Panda, S.K., Dehengia, A. and Kar, V.R. (2016), “Vibration analysis of functionally graded carbon nanotube reinforced composite plate in thermal environment”, *J. Sandw. Struct. Mater.*, **18**(2), 151-173. https://doi.org/10.1177/1099636215613324.
Mesbah, H.A. and Benzaid, R. (2017), “Damage-based stress-strain model of RC cylinders wrapped with CFRP composites”, *Adv. Concrete Constr.*, **5**(5), 539. https://doi.org/10.12989/acc.2017.5.5.539.
Moazzez, K., Saeidi Googarchin, H. and Sharifi, S.M.H. (2018), “Natural frequency analysis of a cylindrical shell containing a variably oriented surface crack utilizing line-spring model”, *Thin Wall. Struct.*, **125**, 63-75. https://doi.org/10.1016/j.tws.2018.01.009.
Najafizadeh, M.M. and Isvandzibaei, M.R. (2007), “Vibration of (FGM) cylindrical shells based on higher order shear deformation plate theory with ring support”, *Acta Mechanica*, **191**, 75-91. http/10.1007/s00707-006-0438-0.
Padovan, J. (1975), “Travelling waves vibrations and buckling of rotating anisotropic shells of revolution by finite element”, *Int. J. Solid Struct.*, **11**(12), 1367-1380. https://doi.org/10.1016/0020-7683(75)90064-5.
Penzes, R.L.E. and Kraus, H. (1972), “Free vibrations of pre-stresses cylindrical shells having arbitrary homogeneous boundary conditions”, *AIAA J.*, **10**, 1309. https://doi.org/10.2514/3.6605.
Ramteke, P.M. (2019), “Effect of grading pattern and porosity on the eigen characteristics of porous functionally graded structure”, *Steel Compos. Struct.*, **33**(6), 865-875. https://doi.org/10.12989/scs.2019.33.6.865.
Ramteke, P.M. and Panda, S.K. (2021), “Free vibrational behaviour of multi-directional porous functionally graded structures”, *Arab. J. Sci. Eng.*, **46**(8), 7741-7756. https://doi.org/10.1007/s13369-021-05461-6.
Ramteke, P.M., Mahapatra, B.P., Panda, S.K. and Sharma, N. (2020), “Static deflection simulation study of 2D Functionally graded porous structure”, *Mater. Today Proc.*, **33**, 5544-5547. https://doi.org/10.1016/j.matpr.2020.03.537.
Ramteke, P.M., Mehar, K., Sharma, N. and Panda, S.K. (2021), “Numerical prediction of deflection and stress responses of functionally graded structure for grading patterns (power-law, sigmoid, and exponential) and variable porosity (even/uneven)”,

Scientia Iranica, **28**(2), 811-829. https://doi.org/10.24200/sci.2020.55581.4290.

Ramteke, P.M., Patel, B. and Panda, S.K. (2020), "Time-dependent deflection responses of porous FGM structure including pattern and porosity", *Int. J. Appl. Mech*., **12**(09), 2050102. https://doi.org/10.1142/S1758825120501021.

Saito, T. and Endo, M. (1986), "Vibrations of finite length rotating cylindrical shell", *J. Sound Vib*., **107**, 17. https://doi.org/10.1016/0022-460X(86)90279-8.

Samadvand, H. and Dehestani, M. (2020), "A stress-function variational approach toward CFRP-concrete interfacial stresses in bonded joints", *Adv. Concrete Constr*., **9**(1), 43-54. https://doi.org/10.12989/acc.2020.9.1.043.

Sewall, J.L. and Naumann, E.C. (1968), *An Experimental and Analytical Vibration Study of Thin Cylindrical Shells with and without Longitudinal Stiffeners*, National Aeronautic and Space Administration, Springfield.

Sharma, P., Singh, R. and Hussain, H. (2019), "On modal analysis of axially functionally graded material beam under hygrothermal effect", *Proceedings of the Institution of Mechanical Engineers, Part C: Journal of Mechanical Engineering Science*, https://doi.org/10.1177/0954406219888234.

Sivadas, K.R. and Ganesan, N. (1964), "Effect of rotation on vibrations of moderately thin cylindrical shell", *J. Vib. Acoust.*, **116**(1),198-202. https://doi.org/10.1115/1.2930412.

Srinivasan, A.V and Luaterbach, G.F. (1971), "Travelling waves in rotating cylindrical shells", *Trans. ASME J. Eng. Indust*., **93**, 1229-1232. https://doi.org/10.1115/1.3428067.

Suresh, S. and Mortensen, A. (1997), "Functionally gradient metals and metal ceramic composites", *Part 2 Therm. Mech. Behav. Int. Mater*, **42**, 85-116. https://doi.org/10.1179/imr.1997.42.3.85.

Swaddiwudhipong. S., Tian. J. and Wang C.M. (1995), "Vibration of cylindrical shells with ring supports", *J. Sound Vib*., **187**(1), 69-93. https://doi.org/10.1006/jsvi.1995.0503.

Wang S.S. and Chen, Y. (1974), "Effects of rotation on vibrations of circular cylindrical shells", *J. Acoust. Soc. Am*., **55**, 1340-1342. https://doi.org/10.1121/1.1914708.

Zhang. X.M., Liu. G.R. and Lam, K.Y. (2001), "Coupled vibration of fluid-filled cylindrical shells using the wave propagation approach", *Appl. Acoust*., **62**, 229-243. https://doi.org/10.1016/S0003-682X(00)00045-1.

Zohar, A. and Aboudi, J. (1973), "The free vibrations of thin circular finite rotating cylinder", *Int. J. Mech. Sci*., **15**, 269-278. https://doi.org/10.1016/0020-7403(73)90009-X.

CC